Journal of Computer-Aided Molecular Design, 2 (1988) 259–266
ESCOM

J-CAMD 054

Computer simulation study of the binding of an antiviral agent to a sensitive and a resistant human rhinovirus

Terry P. Lybrand[a] and J. Andrew McCammon[b]

[a]*Department of Medicinal Chemistry and Supercomputer Institute, University of Minnesota, Minneapolis, MN 55455, U.S.A.*
[b]*Department of Chemistry, University of Houston, Houston, TX 77004, U.S.A.*

Received 15 June 1988
Accepted 8 August 1988

Key words: Molecular dynamics; Thermodynamic cycle–perturbation method; Binding free energy; Human rhinovirus; Antiviral agent binding

SUMMARY

Molecular dynamics simulations have been used to study the free energy of binding of an antiviral agent to the human rhinovirus HRV-14 and to a mutant in which a valine residue in the antiviral binding pocket is replaced by leucine. The simulations predict that the antiviral should bind to the two viruses with similar affinity, in apparent disagreement with experimental results. Possible origins of this discrepancy are outlined. Of particular importance is the apparent need for methods to systematically sample all significant conformations of the leucine side chain.

INTRODUCTION

We present calculations to assess the effect of point mutations in the human rhinovirus-14 (HRV-14) coat proteins on the binding free energy of an antiviral compound (Fig. 1). Specifically, we have used thermodynamic cycle–perturbation [1, 2] calculations to compute the relative binding free energy for the antiviral molecule to wild-type and one mutant HRV-14 coat protein species. The amino acid substitution studied here involves the mutation of valine-188 in the VP1 coat protein to a leucine. This amino acid lies in the antiviral drug binding pocket region of VP1 [3]. In our calculations, we have computed the relative free energy of binding for wild-type and mu-

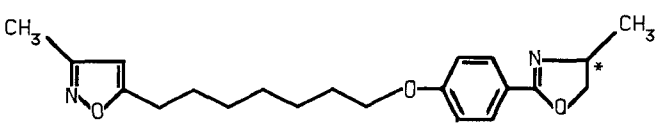

Fig. 1. The antiviral molecule. The (*S*) stereoisomer has been used in all calculations.

0920-654X/89/$3.50

tant structures by 'perturbing' the valine residue into a leucine during the course of a molecular dynamics simulation. Thus, our calculations represent the computer simulation analogue of a point mutation experiment and allow the direct calculation of the relative binding energy of interest.

METHODS

Use of the thermodynamic cycle–perturbation method to compute relative free energies of binding for various ligands to a single receptor site has been described elsewhere [4]. The binding of different antivirals to HRV-14 has been explored in preliminary calculations of this kind [5]. The method also makes possible the introduction of changes to the receptor site, thus permitting the calculation of relative free energies of binding for one ligand to wild-type and 'mutant' receptor proteins [6, 7]. A schematic for the computations is given below:

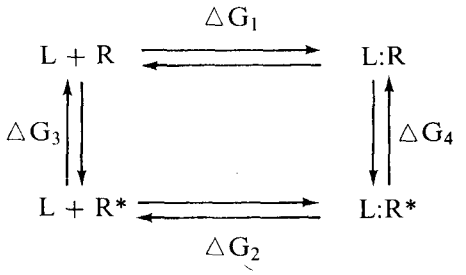

where L is the ligand, R is the wild-type receptor protein, and R* is the mutant receptor protein. The relative free energy of binding for L to wild-type and mutant proteins is

$$\Delta\Delta G = \Delta G_4 - \Delta G_3 = \Delta G_2 - \Delta G_1$$

since the Gibbs free energy is a thermodynamic state function. Calculation of the physically realistic free energy changes ΔG_1 and ΔG_2 requires (1) the definition of a sensible reaction coordinate for each process and (2) molecular dynamics simulations of sufficient length to sample adequately the conformational changes and solvent rearrangement that must occur during complex formation. For biomacromolecular systems, it is seldom possible to satisfy either of these requirements. It is much easier computationally to determine $\Delta\Delta G$ by calculating energy changes for the nonphysical perturbation processes ΔG_3 and ΔG_4, since conformational fluctuations and solvent rearrangement are less dramatic for the perturbations, and no reaction coordinate need be defined.

In these calculations, the perturbation implemented was the transformation of valine-188 in the VP1 coat protein to leucine. Since this is a (potentially) rather significant perturbation in terms of its structural and energetic consequences, a two-step simulation was used to insure that adequate sampling could be performed. The first step involved the mutation of valine to a hybrid species (INX), and the second step completed the mutation to the leucine residue, as shown in the following scheme.

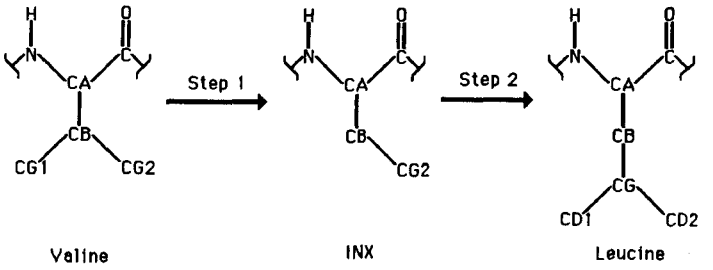

To further enhance the sampling efficiency, van der Waals and electrostatic contributions were computed in separate dynamics simulation runs for each step of each reaction, and 3 – 5 independent determinations for each free energy component (i.e., electrostatic or Lennard–Jones terms) were performed. Each independent determination was started from a different initial configuration for the system, with free energy sampling invoked only after an equilibration period of 30–50 ps. In total, the evaluation of $\triangle\triangle G$ entailed approximately 30 molecular dynamics perturbation simulations, ranging in length from 15 – 60 ps, excluding equilibration periods (approximately 30 ps).

The system consisted of one protomeric unit of the HRV-14 coat protein assembly (proteins VP1, VP2, VP3, and VP4; see Ref. 3, plus a portion of the coat proteins from surrounding protomeric units. Approximately 2000 water molecules were layered over the protein surface and the antiviral molecule was included in the calculation of $\triangle G_4$, yielding a molecular complex of about 12000 atoms. An active site region was defined as all residues within 15 Å of the valine-leucine mutation site. All atoms in the active site region were allowed to move during the simulation, while the remainder of the coat protein structure was kept fixed at initial X-ray positions; all water molecules were permitted to move freely during the simulations. Potential energy function parameters for the amino acid residues were taken from Weiner et al. [8] and the SPC water model was used [9]. Partial charges for the drug molecule were derived according to the method of Singh and Kollman [10] using a 6-31G* basis set in the ab initio calculations. Covalent and Lennard-Jones parameters for the drug molecule were taken from Weiner et al [8] or were determined from ab initio calculations and empirical fitting to spectroscopic data (in the case of several dihedral force constants, see Tables 1 and 2, and Fig. 2). The continuous, or 'slow-growth', free energy perturbation option of the AMBER molecular dynamics program was employed for these calculations [11]. The SHAKE algorithm [12] was used to constrain bonds at equilibrium values and hydrogen masses were increased to 10 AMU [13]. These simulation 'tricks' enhance sampling efficiency but do not affect equilibrium thermodynamic properties. A 9 Å residue-based non-bonded cutoff distance and a 2 fs integration time step were used, with non-bonded pair lists updated once every 20 integration steps. All calculations were performed on Cray X-MP or Cray-2 supercomputers, and graphical analyses were performed with MIDAS [14] and MMS [15] interactive graphics programs on IRIS 3030 and 4D/70G workstations.

RESULTS AND DISCUSSION

The computed value of $\triangle\triangle G$ for the antiviral molecule binding to wild-type virus and the leucine mutant favors the mutant structure by approximately 0.5 kcal/mol. The statistical uncertain-

TABLE I
ATOM LABELS, ATOM TYPES, AND PARTIAL CHARGES FOR THE ANTIVIRAL COMPOUND (SEE FIG. 2 FOR LABELING SCHEME) AND HYBRID AMINO ACID INX

Label	Type	Charge
Antiviral molecule		
O1	OS	−0.1120
N2	NB	−0.4856
C3	CC	0.7795
C31	C3	−0.1462
C4	CJ	−0.5394
C5	CS	0.5541
C6	C2	−0.0159
C7	C2	0.0100
C8	C2	−0.0100
C9	C2	0.0000
C10	C2	−0.0100
C11	C2	0.0100
C12	C2	0.1653
O13	OS	−0.3692
C14	CA	0.4645
C15	CD	−0.1606
C16	CD	0.1787
C17	CD	−0.1606
C18	CD	0.1787
C19	CA	−0.4977
C20	CV	0.8319
N21	NB	−0.6742
C22	CO	0.4650
C23	C3	−0.1518
C24	C2	0.1347
O25	OS	−0.4242
INX		
N	N	−0.5200
H	H	0.2480
CA	CH	0.2040
CB	C2	0.0330
CG2	C3	0.0090
C	C	0.5260
O	O	−0.5000

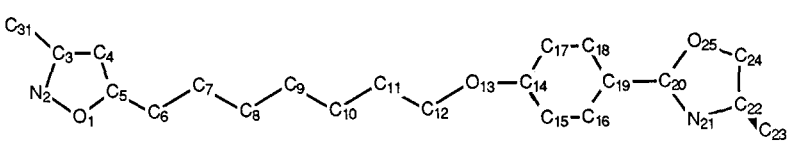

Fig. 2. Atom labeling scheme for the antiviral molecule.

TABLE 2
PARAMETERS FOR THE ANTIVIRAL MOLECULE NOT INCLUDED IN REF. 8. K_b, K_a, and K_d ARE FORCE CONSTANTS AND R_b, Θ_a, AND γ ARE EQUILIBRIUM GEOMETRY VALUES FOR BONDS, ANGLES, AND DIHEDRAL ANGLES, RESPECTIVELY, WHILE N IS THE PHASE OF THE DIHEDRAL ANGLE

Bonds	K_b(kcal/mol/Å^2)	R_b(Å)
OS-NB	320.	1.410
OS-CS	440.	1.360
CC-C3	350.	1.485
CC-CJ	478.	1.394
CJ-CS	564.	1.340
CS-C2	349.	1.460
OS-CA	320.	1.440
CA-CV	357.	1.480
CV-NB	546.	1.291
CV-OS	320.	1.408
NB-CO	424.	1.383
CO-C3	260.	1.510
Angles	**K_a(kcal/mol/rad^2)**	**Θ_a(degrees)**
OS-NB-CC	70.	105.7
OS-CS-CJ	80.	108.8
OS-CS-C2	80.	116.4
NB-CC-C3	70.	119.6
NB-CC-CJ	70.	111.2
NB-OS-CS	100.	108.1
CC-CJ-CS	70.	106.0
C3-CC-CJ	70.	120.0
CJ-CS-C2	70.	120.0
CS-C2-C2	70.	109.5
C2-OS-CA	100.	109.5
OS-CA-CD	70.	120.0.
CD-CA-CD	70.	120.0.
CA-CV-NB	70.	124.8
CA-CV-OS	70.	124.9
CV-NB-CO	70.	106.8
CV-OS-C2	100.	112.5
NB-CO-C2	80.	111.5
NB-CV-OS	70.	110.3
CO-C2-OS	80.	109.5
C3-CO-C2	70.	109.5
Dihedrals	**n**	**K_d(kcal/mol)**	**γ(degrees)**
X-CJ-CS-X	2	28.4	180
X-CS-C2-X	6	0.0	0
X-OS-CS-X	2	3.5	180
X-CC-CJ-X	2	5.5	180
X-NB-OS-X	1	2.9	180
X-OS-CA-X	2	1.8	180
X-CA-CV-X	4	3.0	180
X-CV-NB-X	2	24.2	180
X-CV-OS-X	2	4.6	180
X-NB-CO-X	2	5.8	0
X-C2-CO-X	2	4.8	180

ty in the computed results (± 2.5 kcal/mol) is large relative to the free energy difference, so it is possible to suggest only that there is no marked preference for the antiviral to bind to wild-type or leucine mutant, based on these calculations. The free energy changes for each step in the perturbation process are given in Table 3. Based on preliminary analyses of energetics and structures, there is no evidence of serious steric strain in either the drug-virus complex or the free virus (T. Lybrand, unpublished; cf. also Ref. 16).

Early graphical analysis suggests that the leucine mutation introduces small, localized conformational changes in the drug-virus complex. Several dihedral angles in the alkyl chain of the drug molecule (e.g. in particular, angles C7-C8-C9-C10 and C8-C9-C10-C11) exhibit transitions from trans (i.e., X-ray) conformations to gauche$^+$ conformations. This is consistent with the marked flexibility of this chain observed in other simulations of the HRV-14–antiviral complex [17, 18]. The only other noticeable conformational changes for the complex involve small shifts (e.g., <0.5 Å) in protein backbone atoms of VP1 (residues 186–191) and small fluctuations (± 30°) for the X2 torsion angle of phenylalanine-186 in VP1. These dihedral angle rearrangements in the drug molecule and localized small shifts of the protein backbone permit introduction of the leucine side chain without steric conflict. The leucine side chain introduced at residue 188 of VP1 displays two 'average' side-chain conformations in the drug–virus complex calculations (X1, X2 are g^+, g^- or g^-, g^+).

The structures from the free virus mutation calculations likewise show little deviation from the X-ray structure for the wild-type virus in the region of the mutation. There is a shift in protein

TABLE 3
COMPUTED RESULTS FOR $\triangle G_4$ (DRUG–VIRUS COMPLEX) AND $\triangle G_3$ (FREE VIRUS)*

Step 1 (Valine > INX)	Step 2 (INX > Leucine)
Drug–virus complex	
2.190 kcal/mol (2.009; 0.025)	−0.948 kcal/mol (−1.258; 0.310)
2.317 kcal/mol (1.982; 0.335)	−0.341 kcal/mol (−0.497; 0.156)
2.179 kcal/mol (2.152; 0.027)	−0.643 kcal/mol (−0.917; 0.274)
0.460 kcal/mol (0435; 0.025)	−0.186 kcal/mol (−0.433; 0.247)
	−0.019 kcal/mol (−0.266; 0.247)
Average: 1.8 ± 0.9 kcal/mol	Average: −0.43 ± 0.4 kcal/mol
$\triangle G_4$ = step 1 + step 2 ≈ 1.4 kcal/mol	
Free virus	
0.142 kcal/mol (0.114; 0.023)	1.202 kcal/mol (0.914; 0.288)
1.135 kcal/mol (1.119; 0.016)	0.320 kcal/mol (0.059; 0.261)
1.734 kcal/mol (1.703; 0.031)	0.958 kcal/mol (0.543; 0.415)
1.411 kcal/mol (1.150; 0.261	
Average: 1.1 ± 0.7 kcal/mol	Average: 0.83 ± 0.5 kcal/mol
$\triangle G_3$ = step 1 + step 2 ≈ 1.9 kcal/mol	

*The numbers in brackets indicate the Lennard–Jones and electrostatic contributions, respectively, for each calculated free energy value. Error bars indicate the standard deviation of results for each step.

backbone atoms of VP1 (residues 186–191) that is somewhat larger than that observed in the drug–virus complex (~ 1Å), but the side-chain conformations in the region of the point mutation are essentially unchanged from the X-ray structure. The leucine introduced at position 188 again displays a variety of side-chain conformations in the perturbation calculations (X1 is g^+, X2 is g^- or g^+).

In both the free virus and the drug–virus complex, side chains that are exposed to solvent at the surface show much larger fluctuations during the calculations, and larger deviations from the original X-ray positions. These conformational fluctuations appear to be due in large part to solvent collisions against the protein surface. Otherwise, there is little noticeable difference between X-ray and 'average' simulated viral protein structures. More detailed analysis of both the energetic and structural data is necessary to confirm these preliminary observations.

This result (i.e., the antiviral molecule binds approximately equally well to the mutant protein and the wild-type protein) appears to be inconsistent with available biological data, which suggest that the leucine mutation drastically diminishes the antiviral activity of the antiviral molecule [16]. However, the result is quite sensible when compared to qualitative graphical analysis and simple model building experiments for the mutant structures, using the wild-type X-ray structures as a reference. These are several possible explanations for this discrepancy between experiment and simulation results. The simulation models assume a uniform binding orientation for the antiviral molecule to both wild-type and mutant forms, and any deviation from this assumption, such as a mixed binding mode for the drug molecules, may have significant consequences for the computed binding free energy. It may be that the reduction of antiviral activity displayed by the antiviral molecule against the leucine mutant is not due to a diminution of intrinsic drug–protein affinity, but rather that the mutation reduces drug activity in some other fashion. For example, biological efficacy may reflect the kinetics of binding or specific interactions between the antiviral molecule and the protein capsid as well as the binding equilibrium. It is also possible that the computed relative free energy of binding is misleading due to the failure of the simulations to sample the relevant conformational states of the mutant protein. This is, in fact, a particularly likely difficulty. Preliminary analysis suggests that the computed free energy changes may be quite sensitive to the conformation of the leucine side chain. Despite the number and lengths of the simulations performed here (see Table 3), only a few of the possible conformations of this side chain were sampled. This makes clear that new methods for systematically sampling conformations and properly combining the corresponding free energies are needed. Such methods are currently being developed.

ACKNOWLEDGEMENTS

We are indebted to Professor Montgomery Pettitt and Dr. Wan Lau for their assistance in the calculation of energy parameters for the antiviral agent, to Professor Michael Rossmann and Dr. John Badger for communicating X-ray coordinates and manuscript drafts before publication, and to Dr. Adi Treasurywala and Dr. Frank Dutko for helpful suggestions.

This work has been supported in part by grants from the National Science Foundation, the Robert A. Welch Foundation, the Sterling–Winthrop Research Institute, the Minnesota Supercomputer Institute, and Cray Research, Inc. T.P.L. is the recipient of a Presidential Young Investigator Award from NSF and a Searle Scholars Award from the Searle Scholars Program/The

Chicago Community Trust. J.A.M. is the recipient of the 1987 Hitchings Award from the Burroughs Wellcome Fund.

REFERENCES

1 McCammon, J.A., Science, 238 (1987) 486–491.
2 McCammon, J.A. and Harvey, S.C. 'Dynamics of Proteins and Nucleic Acids', Cambridge University Press, Cambridge, 1987.
3 Smith, T.J., Kremer, M.J., Luo, M., Vriend, G., Arnold, E., Kamer, G., Rossmann, M., McKinley, M.A., Diana, G.D., Otto, M.J., Science, 233 (1986) 1286–1293.
4 Lybrand, T.P., McCammon, J.A., and Wipff, G., Proc. Natl. Acad. Sci. U.S.A., 83 (1986) 833–835.
5 Lybrand, T.P., Lau, W.F., McCammon, J.A., and Pettitt, B.M., In D. Oxender (Ed.), Protein Structure, Folding, and Design 2, Alan R. Liss, New York, 1987, p. 227–233.
6 Wong, C.F. and McCammon, J.A., J. Am. Chem. Soc., 108 (1986) 3830–3832.
7 Rao, S.N., Singh, U.C., Bash, P.A., and Kollman, P.A., Nature, 328 (1987) 551–554.
8 Weiner, S.J., Kollmanm, P.A., Case, D.A., Singh, U.C., Ghio, C., Alagona, G., Profeta, S., and Weiner, P., J. Am. Chem. Soc., 106 (1984) 765–784.
9 Berendsen, H.J.C., Postman, J.P.M., and van Gunsteren W.F., In Pullman, B. (Ed.), Intermolecular Forces, Reidel, Dordrecht, 1981, p. 331–342.
10 Singh, U.C. and Kollman, P.A., J. Comput. Chem., 5 (1984) 129–145.
11 Singh, U.C., Weiner, P.K., Caldwell, J., and Kollman, P.A., AMBER 3.0 UCSF, 1986.
12 Ryckaert, J.P., Ciccotti, G., and Berendsen, H.J.C., J. Comput. Phys., 23 (1977) 327–341.
13 Wood, D.W., In Franks F. (Ed.) Water: A comprehensive Treatise, Vol. 6, Plenum, New York, 1979.
14 Gallo, L., Huang, C., Ferrin, T. and Langridge, R., MIDAS USCF, 1983.
15 Dempsey, S., MMS UCSD, 1985.
16 Badger, J., Minor, I., Kremer, M.J., Oliveira, M.A., Smith, T.J., Griffith, J.P., Guerin, D.M.A., Krishnaswamy, S., Luo, M., Rossmann, M.G., McKinlay, M.A., Diana, G.D., Dutko, F.J., Fancher, M., Rueckert, R.R. and Heinz, B.A., Proc. Natl. Acad. Sci. U.S.A., 85, 3304–3308.
17 Lau, W.F., Pettitt, B.M. and Lybrand, T.P., Mol. Simul., in press.
18 Lau, W.F. and Pettitt, B.M., to be published.